Fluorescence fluctuations from a multilevel atom in a nonstationary phase-diffusion field: Deterministic frequency modulation

James Camparo
Electronics and Photonics Laboratory, The Aerospace Corporation, P. O. Box 92957, Los Angeles, California 90009, USA
(Received 2 July 2003; published 8 January 2004)

It is well known that a field's quantum noise can have a profound effect on the fluctuations of laser-induced fluorescence (LIF). However, though previous studies have led to a good understanding of this process in the case of stationary fields, many of the important applications of LIF employ some form of laser modulation, yielding a field of nonstationary stochastic character. Here, we discuss the results from numerical experiments that examine the influence of a nonstationary field on the LIF noise. Specifically, we consider a phase-diffusion field and LIF from a beam of alkali-metal-like atoms with ground and excited-state Zeeman splitting when the field undergoes deterministic frequency modulation. Our computational results show that deterministic modulation at high Fourier frequencies (i.e., 10 MHz) can significantly increase the LIF noise at low Fourier frequencies (e.g., 1 Hz), and that the amount of LIF noise amplification depends on a complicated interplay among the laser's linewidth, the modulation frequency, the modulation index, and the multilevel atomic system's energy-level spacing. Interestingly, we find that certain values of the atom's Zeeman splitting significantly decrease the magnitude of LIF noise.

DOI: 10.1103/PhysRevA.69.013802 PACS number(s): 42.62.Fi, 42.50.Gy, 32.50.+d, 32.80.−t

I. INTRODUCTION

For quite some time, researchers have known that the coherence characteristics of a radiation field have important consequences for the basic field–atom interaction [1]. Initially, studies of the stochastic-field–atom problem focused on relatively straightforward quantities; finding, for example, that a singlemode laser's quantum noise not only influenced the widths and amplitudes of the Mollow fluorescent triplet [2], but also the triplet's asymmetry [3]. However, starting around the late 1980's, theoretical and experimental attention began to turn towards more complex issues. For example, in a careful study comparing theory and experiment Anderson *et al.* [4] examined the variance of laser-induced fluorescence (LIF) from an atomic beam, while Camparo and Lambropoulos found that correlated frequency and amplitude fluctuations give rise to resonant frequency shifts [5]. Additionally, Yabuzaki *et al.* [6] showed that when a laser beam passes through a resonant medium, the high-frequency Fourier spectrum of transmitted laser-intensity fluctuations ($\sim$ GHz regime) carries detailed information on the medium's energy level structure, and that this effect can be used as a new type of high-resolution spectroscopy [7]. Yabuzaki's "phase-noise (PM) to amplitude-noise (AM)" conversion process is also significant at very low Fourier frequencies ($\leqslant$1 Hz) [8,9], where it plays an important role in limiting the performance of laser-pumped atomic clocks [10].

Notwithstanding the progress that has been made in understanding the stochastic-field–atom interaction over the past years, in a number of these studies the field has corresponded to a stationary stochastic process [11]. In particular, in most previous studies of LIF fluctuations the (stochastically averaged) detuning of the field from resonance was independent of time. However, in many areas of spectroscopy the mean frequency of a resonant field is modulated [12] in order to improve the signal-to-noise ratio [13,14] or to stabilize the field's emission wavelength [15]. Here, we consider the problem of LIF from a beam of alkali-metal-like atoms with nuclear spin $\frac{1}{2}$ through numerical experiments, when the finite-linewidth single mode field exciting the atoms undergoes deterministic frequency modulation. Though as noted above, previous studies have shown that the laser's phase fluctuations induce fluorescence intensity fluctuations, our focus here is on the manner in which nonstationarity can amplify this effect; in particular, how rapid modulation affects fluorescence noise at very low Fourier frequencies. This question has particular relevance to double-resonance spectroscopy, trace detection, and laser cooling and trapping experiments, where the laser's phase is modulated rapidly for purposes of wavelength stabilization and the atomic signal is averaged over some long time interval. We note that in state-of-the art atomic clocks, laser state preparation and state detection are of paramount significance, and recent experimental results suggest that the performance of these devices may be influenced by an interplay between the laser's deterministic modulation and the stochastic-field–atom interaction [16].

As will be discussed more fully below, we quantify the fluorescence noise in terms of the fluorescence fluctuations' Allan deviation [17] $\sigma_{\Delta F/F}(\tau)$ at averaging times τ on the order of one second; and investigate the manner in which the signal-to-noise (S/N) ratio of LIF depends on modulation frequency, modulation index, and Zeeman splitting. In the following section, we develop an adiabatic approximation to the modulated, stochastic-field–atom interaction problem, which assumes that the deterministic and stochastic frequency fluctuations of a phase-diffusion field are slow compared to the atom's intrinsic response time. The purpose of this approximate theory is to provide a conceptual framework for the interpretation of the more accurate numerical results presented later. Then in Sec. III, we outline our model alkali-metal-like system and the stochastic density-matrix

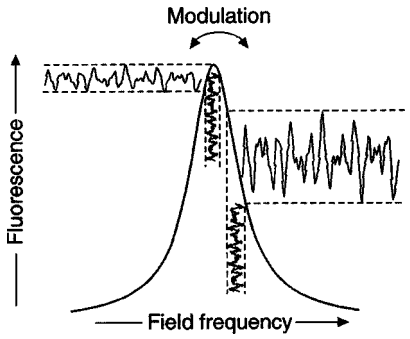

FIG. 1. Conceptual illustration showing the manner in which deterministic frequency modulation can influence LIF noise in the adiabatic limit of the atom's response. On a time scale that is short compared to the modulation period, the stochastic frequency (i.e., phase) fluctuations of the laser give rise to stochastic fluorescence fluctuations, and these have an ''instantaneous'' variance that depends on the field and atom detuning at some particular moment. Due to the nonlinear nature of the atom's response to the field, the instantaneous variance is modulated, and this gives rise to nonstationary fluorescence fluctuations, more specifically wide sense, periodically stationary fluorescence fluctuations. Consequently, if the fluorescence is averaged over a time that is long compared to the modulation period, the averaged fluorescence will appear to have the character of a stationary process whose variance depends on the modulation depth of the field and the atomic linewidth.

equations that we solve in order to generate a time series of simulated fluorescence fluctuations. (Details on the numerical approach are discussed in an appendix.) Results will be presented in Sec. IV and interpreted using the adiabatic approximation. We conclude with a summary of our findings and a brief discussion of their significance for precision laser spectroscopy.

II. THE ADIABATIC APPROXIMATION

Prior to discussing the results from the detailed numerical computations, it is useful to have some conceptual framework in which to understand those results. Therefore, in this section we develop a semiquantitative theory of the modulated, stochastic-field–atom interaction problem, emphasizing that the theory is primarily of interpretive value. Briefly, if we assume that the deterministic and stochastic frequency variations of the field are in some sense slow, then the atom's basic interaction with the field will be independent of those fluctuations to first order. This is illustrated conceptually in Fig. 1, where the ''instantaneous'' variance of fluorescence fluctuations (i.e., the variance over a very short time interval), arising from the laser's instantaneous frequency noise, varies periodically as the laser is modulated about resonance.

To develop the adiabatic approximation, we consider the two-level atom density-matrix equations in the rotating frame (and with the rotating-wave approximation), where $\Delta(t)$ is a time-dependent field/atom detuning and Ω is a constant Rabi frequency

$$\dot{\sigma}_{22}+\gamma_1\sigma_{22}-\mathrm{Im}[\sigma_{21}\Omega^*]=0, \tag{1a}$$

$$\dot{\sigma}_{21}+[\gamma_2+i\Delta(t)]\sigma_{21}+\frac{i\Omega}{2}(\sigma_{22}-\sigma_{11})=0. \tag{1b}$$

Here, the σ_{ij}'s are the density-matrix elements, γ_1 and γ_2 are the longitudinal and transverse relaxation rates, respectively, and we have $\Delta(t)=\Delta_0+m\omega_m\sin(\omega_m t)+\delta(t)=\tilde{\Delta}(t)+\delta(t)$, where m is the modulation index, ω_m the modulation frequency, and $\delta(t)$ the mean-zero random frequency fluctuations.

Since our interest is in the density-matrix behavior when the atoms are in equilibrium with the fluctuating field, we would like to set the first terms on the left-hand side of Eqs. (1) to zero. In order to understand the conditions under which this is reasonable, we write the equilibrium density-matrix elements approximately as

$$\sigma_{ij}(t)\cong\Sigma_{ij}+A\sin(\omega_m t+\theta)+\delta(t)\left.\frac{d\tilde{\sigma}_{ij}(t)}{d\tilde{\Delta}}\right|_{\tilde{\Delta}}, \tag{2}$$

where $\tilde{\sigma}_{ij}(t)\equiv\Sigma_{ij}+A\sin(\omega_m t+\theta)$. In essence, we arrive at Eq. (2) by assuming that we can write the temporal evolution of the density matrix as the sum of a deterministic component and a stochastic component. We obtain the deterministic component from the first-order terms of a Fourier expansion, and the stochastic component by expanding $\tilde{\sigma}_{ij}$ in a Taylor series about the instantaneous detuning $\tilde{\Delta}$, assuming that the $\delta(t)$ are in some sense small [18]. Notice that in writing Eq. (2) we have already invoked an adiabatic approximation, since we assume that the frequency fluctuations have little effect on the evolution of σ_{ij}, and that a Taylor series expansion using $\tilde{\sigma}_{ij}$ has meaning. Since $\dot{\Sigma}_{ij}=0$ by definition,

$$\dot{\sigma}_{ij}(t)\cong A\omega_m\cos(\omega_m t+\theta)+\dot{\delta}(t)\left.\frac{d\tilde{\sigma}_{ij}(t)}{d\tilde{\Delta}}\right|_{\tilde{\Delta}}+\delta(t)\left.\frac{d\dot{\tilde{\sigma}}_{ij}(t)}{d\tilde{\Delta}}\right|_{\tilde{\Delta}}. \tag{3}$$

Comparing the terms in Eq. (3) to $\gamma_{1,2}\sigma_{ij}$, which determines the minimum rate of density-matrix evolution on the left-hand side of Eqs. (1), we can ignore the first term on the right-hand side of Eq. (3) under the (deterministic) adiabatic approximation $\omega_m\ll\gamma_{1,2}$. This, of course, means that $\dot{\tilde{\sigma}}_{ij}$ is small, and hence that the last term on the right-hand side of Eq. (3) can also be ignored, at least for fields with reasonably small (effective) rms values of δ (i.e., narrow-linewidth fields) [18]. Consequently, under a deterministic adiabatic approximation $\dot{\sigma}_{ij}$ should have a magnitude of at most $\dot{\delta}(t)\,d\tilde{\sigma}_{ij}(t)/d\tilde{\Delta}\,|_{\tilde{\Delta}}$.

In order to estimate the magnitude of this term, we first recognize that $d\tilde{\sigma}_{ij}(t)/d\tilde{\Delta}\,|_{\tilde{\Delta}}$ should be of order $(\gamma_2^2+\Omega^2)^{-1/2}$. Further, given that the time scale of the field-atom coupling is on the order of a Rabi period, we estimate the magnitude of $\dot{\delta}$ as $\Omega\sqrt{\langle\delta_\Omega^2\rangle}$, where $\sqrt{\langle\delta_\Omega^2\rangle}$ is the root-mean-square value of the field's frequency fluctuations

within a bandwidth Ω. In other words, since the atom will not respond to fluctuations that occur on a time scale much faster than the Rabi period, the maximum rate of δ having significant affect on atomic evolution should be on the order of a time-averaged rms value of the frequency fluctuations (i.e., $\sqrt{\langle \overline{\delta_\Omega^2} \rangle}$) per Rabi period (i.e., per Ω^{-1}).

In the case that the field corresponds to a phase-diffusion, singlemode laser, we have [19]

$$\langle \delta(t)\,\delta(t+\tau)\rangle = \gamma_L \beta e^{-\beta|\tau|}, \tag{4}$$

where γ_L is the (essentially) Lorentzian laser linewidth (full width at half maximum) and β is the bandwidth of the field's frequency fluctuations [20]. Thus,

$$\langle \overline{\delta_\Omega^2} \rangle = \frac{\gamma_L \beta^2}{\pi} \int_{-\Omega/2}^{\Omega/2} \frac{d\omega}{\beta^2+\omega^2} = \frac{2}{\pi}\gamma_L \beta \tan^{-1}\left(\frac{\Omega}{2\beta}\right). \tag{5}$$

Since in general we expect $\beta \gg \Omega$ (for example, in the case of a single mode diode laser $\beta \sim 10^3$ MHz while $\Omega \sim 10-100$ MHz [21]), Eq. (5) reduces to

$$\langle \overline{\delta_\Omega^2} \rangle \cong \frac{\gamma_L \Omega}{\pi}. \tag{6}$$

Therefore, in order of magnitude we expect

$$\dot{\delta}(t) \left.\frac{d\tilde{\sigma}_{ij}(t)}{d\tilde{\Delta}}\right|_{\tilde{\Delta}} \approx \Omega \sqrt{\frac{\gamma_L \Omega}{\pi(\gamma_2^2+\Omega^2)}}, \tag{7}$$

so that for weak fields (i.e., $\Omega \ll \gamma_2$) and/or sufficiently narrow-linewidth lasers (i.e., $\gamma_L \ll \gamma_2$, Ω) we can ignore this term relative to $\gamma_{1,2}\sigma_{ij}$. Consequently, under fully adiabatic conditions, which we now define as ω_m, $\gamma_L \ll \gamma_2$, we have

$$\gamma_1 \sigma_{22} - \mathrm{Im}[\sigma_{21}\Omega^*] \cong 0, \tag{8a}$$

$$[\gamma_2 + i\Delta(t)]\sigma_{21} + \frac{i\Omega}{2}(\sigma_{22}-\sigma_{11}) \cong 0. \tag{8b}$$

To proceed with the solutions of Eqs. (8), we now employ a perturbation approach [22], writing the density-matrix elements as

$$\sigma_{ij} = \sigma_{ij}^{(0)} + \sigma_{ij}^{(1)} + \sigma_{ij}^{(2)} + \cdots. \tag{9}$$

Basically, we consider the stochastic portion of the field as a separate perturbation on the atom, so that the various terms in Eq. (9) correspond to increasing orders of the stochastic portion's contribution to density-matrix evolution. Substituting Eq. (9) into Eqs. (8) and retaining only terms up to first order in stochasticity, we obtain

$$\gamma_1(\sigma_{22}^{(0)} + \sigma_{22}^{(1)}) = \mathrm{Im}[(\sigma_{21}^{(0)} + \sigma_{21}^{(1)})\Omega^*], \tag{10a}$$

$$[\gamma_2 + i(\tilde{\Delta}+\delta)]\sigma_{21}^{(0)} + (\gamma_2 + i\tilde{\Delta})\sigma_{21}^{(1)} = -\frac{i\Omega}{2}[2(\sigma_{22}^{(0)} + \sigma_{22}^{(1)}) - \sigma_0]. \tag{10b}$$

Here, we have normalized the density matrix so that $\sigma_{22} + \sigma_{11} = \sigma_0$. Equating terms of similar order and carrying through the algebra, we eventually obtain

$$\sigma_{22}^{(1)}(t) = -\delta(t)\kappa(t) = -\delta(t) \times \left[\frac{\sigma_0[\Delta_0 + m\omega_m \sin(\omega_m t)](\gamma_2/\gamma_1)\Omega^2}{(\gamma_2^2 + [\Delta_0 + m\omega_m \sin(\omega_m t)]^2 + (\gamma_2/\gamma_1)\Omega^2)^2}\right]. \tag{11}$$

Note that this is equivalent to the equation we would have obtained by solving Eqs. (1) in the steady state, replacing Δ in the solution with $\tilde{\Delta}$ in order to obtain $\sigma_{22}^{(0)}$, and then defining $\sigma_{22}^{(1)}$ as $\delta(t)\, d\sigma_{22}^{(0)}/d\tilde{\Delta}\,|_{\tilde{\Delta}}$. This is basically the procedure outlined by Kitching *et al.* in their intuitive, ''passive susceptibility'' description of the manner in which laser phase-noise maps onto an atomic system's evolution [23]. From this perspective, the present work clarifies the various approximations that are invoked in the Kitching model. Further, from a statistical point of view, it is worth noting that the sign of $\sigma_{22}^{(1)}$ is really determined by the sign of $\delta(t)$. Consequently, for the nearly white frequency fluctuations of interest here, we reexpress Eq. (11) as $\sigma_{22}^{(1)}(t) = \delta(t)|\kappa(t)|$ to simplify our analysis later.

While Eq. (11) expresses the moment-to-moment fluctuations of σ_{22}, our interest is in the low-frequency behavior of the excited-state population (i.e., fluorescence) fluctuations. We therefore define two new random processes $[\overline{\sigma_{22}^{(1)}(t)}]_\tau$ and $\overline{\delta(t)}_\tau$, which are averages over a relatively long time τ:

$$[\overline{\sigma_{22}^{(1)}(t)}]_\tau \equiv \frac{1}{\tau}\int_{t-\tau/2}^{t+\tau/2} \sigma_{22}^{(1)}(t')dt', \tag{12a}$$

$$\overline{\delta(t)}_\tau \equiv \frac{1}{\tau}\int_{t-\tau/2}^{t+\tau/2} \delta(t')dt'. \tag{12b}$$

Here, τ^{-1} might correspond to the bandwidth limit of a fluorescence measurement system or the bandwidth of a feedback loop in an atomic clock. Employing Eq. (11) in Eq. (12a), we get

$$[\overline{\sigma_{22}^{(1)}(t)}]_\tau \equiv \frac{1}{\tau}\int_{t-\tau/2}^{t+\tau/2} \delta(t')|\kappa(t')|dt' = \frac{1}{\tau}\left\{\int_{t-\tau/2}^{t-\tau/2+T} \delta(t')|\kappa(t')|dt' + \int_{t-\tau/2+T}^{t-\tau/2+2T} \delta(t')|\kappa(t')|dt' + \cdots\right\}, \tag{13}$$

where $T = 2\pi/\omega_m$. However, due to the periodicity of $\kappa(t)$, Eq. (13) can be rewritten as

$$[\overline{\sigma_{22}^{(1)}}(t)]_\tau = \frac{1}{\tau}\int_{t-\tau/2}^{t-\tau/2+T} |\kappa(t')|\{\delta(t')+\delta(t'+T) + \delta(t'+2T)+\cdots+\delta[t'+(\tau/T-1)T]\}dt'. \tag{14}$$

Since in the cases of most general interest the measurement time scale will be much longer than the modulation period (e.g., $\tau \sim 1$ sec, $T \leqslant 10^{-3}$ sec, and $\beta^{-1} \leqslant 10^{-9}$ sec), the term in brackets can be approximated as $(\tau/T)\overline{\delta}_\tau$, which then yields

$$[\overline{\sigma_{22}^{(1)}}(t)]_\tau \approx \frac{\overline{\delta}_\tau}{T}\int_0^T |\kappa(t')|dt' \equiv \overline{\delta}_\tau |\overline{\kappa}|_T. \tag{15}$$

Thus, the variance of $[\overline{\sigma_{22}^{(1)}}(t)]_\tau$, and hence the variance of LIF, is given by the variance of the laser's frequency fluctuations averaged over τ, $\overline{\delta}_\tau$, amplified by the factor $|\overline{\kappa}|_T^2$.

For the case $\Delta_0 = 0$, we have from Eq. (11) for the rms noise of the atom's excited-state population N_0

$$N_0 \equiv \left[\frac{\sqrt{\langle \overline{\delta}_\tau^2\rangle}}{T}\int_0^T |\kappa(t')|dt'\right]_{\Delta_0=0} = \frac{2\sqrt{\langle \overline{\delta}_\tau^2\rangle}}{T}\int_0^{T/2} \frac{\sigma_0(\gamma_2/\gamma_1)\Omega^2 m\omega_m \sin(\omega_m t)}{(\gamma_2^2 + m^2\omega_m^2 \sin^2(\omega_m t) + (\gamma_2/\gamma_1)\Omega^2)^2}dt, \tag{16}$$

which yields after carrying out the integration

$$N_0 = \frac{\sqrt{\langle \overline{\delta}_\tau^2\rangle}\sigma_0}{\pi}\frac{m\omega_m(\gamma_2/\gamma_1)(I/2I_s)A_{eg}^2}{\Gamma^2}\left\{\frac{1}{(\Gamma^2 - m^2\omega_m^2)} + \frac{1}{m\omega_m\Gamma}\tanh^{-1}\left(\frac{m\omega_m}{\Gamma}\right)\right\}, \tag{17a}$$

where $\Gamma^2 \equiv [\gamma_2^2 + m^2\omega_m^2 + (\gamma_2/\gamma_1)(I/2I_s)A_{eg}^2]$. In writing Eq. (17a), we have defined the saturation intensity I_s as $2.5 \times 10^{-28} A_{eg}/\lambda^3$, where A_{eg} is the Einstein-A coefficient in $\sec^{-1}$, λ is the transition wavelength in meters, and I_s is in W/cm^2, so that $\Omega = A_{eg}\sqrt{I/2I_s}$. In situations without modulation, such that $m\omega_m = 0$, the excited-state rms population noise N_Δ is

$$N_\Delta \equiv \left[\frac{\sqrt{\langle \overline{\delta}_\tau^2\rangle}}{T}\int_0^T |\kappa(t')|dt'\right]_{m\omega_m=0} = \frac{\sqrt{\langle \overline{\delta}_\tau^2\rangle}\sigma_0\Delta_0(\gamma_2/\gamma_1)(I/2I_s)A_{eg}^2}{[\gamma_2^2 + \Delta_0^2 + (\gamma_2/\gamma_1)(I/2I_s)A_{eg}^2]^2}, \tag{17b}$$

indicating that $[\overline{\sigma_{22}^{(1)}}(t)]_\tau$, and hence LIF noise, is zero on resonance. Note, however, that Eq. (17b) only accounts for first-order effects in the expansion of Eq. (9); on resonance, higher-order terms in the expansion will yield a finite LIF noise level on resonance.

Examining the general character of the adiabatic solutions, we first note from Eq. (17a) that for $m\omega_m \neq 0$, N_0 always has a finite, potentially large, value, regardless of second-order effects, even when $\tau \gg 2\pi/\omega_m$. Due to our focus on periodically stationary fields, the preceding discussion indicates that averaging over the modulation period produces a wide-sense stationary LIF process from an underlying nonstationary LIF process [assuming, of course, that the $\delta(t)$ are wide-sense stationary]. Further, as suggested by Fig. 1 and quantified by Eq. (11), rapid modulation of the laser frequency results in rapid modulation of the LIF fluctuations' instantaneous variance. However, since most experiments are concerned with time scales much longer than the modulation period, these periodically varying changes in the LIF noise are not observed in the experimental data. Rather, the rms noise of the measured LIF signal corresponds to a weighted mean of the instantaneous LIF variances, with the weighting factor contributing through the time-independent quantity $|\overline{\kappa}|_T$. The second point to note from Eq. (17a) is that the significant modulation parameter is *not* the modulation frequency by itself, but rather the amplitude of the frequency modulation $m\omega_m$. Thus, fields with widely different modulation frequencies will have similar effects if their frequency-modulation amplitudes are equivalent.

III. MODEL SYSTEM DENSITY-MATRIX THEORY

In order to accurately study the multilevel, stochastic-field–atom interaction problem, we now consider the specific case of laser-induced fluorescence from a thermal beam of alkali-metal-like atoms as illustrated in Fig. 2(a), and, in particular, the important special case of LIF associated with the Cs $6^2S_{1/2}(F_g=4) - 6^2P_{3/2}(F_e=5)$ cycling transition that produces a large number of resonantly scattered photons per atom. However, in the case of the real cesium atom (i.e., Cs^{133} with nuclear spin I equal to 7/2) the study of density-matrix evolution could conceivably involve 399 simultaneous, stochastic differential equations, which would have to be repeated for some number (e.g., 10) different atomic velocity groups. Obviously, some simplification of the problem is required in order to make it computationally manageable, and so we have chosen to replace the real cesium atom with a fictitious (stable) $I=1/2$ isotope that nonetheless has the Cs^{133} nuclear magnetic moment [24] such that $F_g = 0,1$ with $\Delta\nu_{\mathrm{HFS}} = 9192.6$ MHz, and $F_e = 1,2$ with $\Delta\nu_{\mathrm{HFS}} = 276.8$ MHz.

We further confine our consideration to a situation in which the laser beam is linearly polarized with its polarization direction perpendicular to the atomic beam's quantization axis. Thus, the laser induces $\Delta m_F = \pm 1$ transitions (i.e., $\pm\sigma$ polarized light). The problem thereby requires the solution of 33 simultaneous, stochastic differential equations (after including the constraint of normalization). As illustrated in Fig. 2(b), the laser induces excited and ground state coherences (shown as dashed lines in the figure) in our fictitious isotope corresponding to two, three, and four-photon transitions. It is worth noting that in the case of the real Cs^{133} atom coherences are generated that correspond to ten-photon transitions. Since, as a general rule, the order of the photon process determines the highest order field-correlation func-

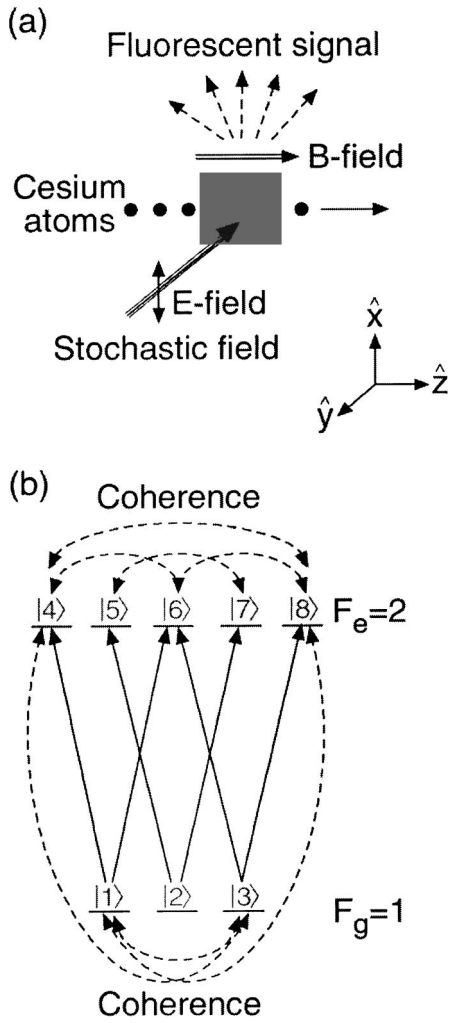

FIG. 2. (a) Illustration of the modeled LIF experiment: cesium atoms travel into and out of a fluorescence detection region and experience a static magnetic field oriented perpendicular to the laser polarization. (b) Illustration of the density matrix couplings that occur in our fluorescence simulation. Solid lines correspond to laser one-photon transitions; dashed lines correspond to coherences that the laser-atom interaction creates.

tion of significance for the stochastic-field–atom interaction, there is the potential for LIF to depend on very high-order correlation functions of the laser field. To include the effects of a static magnetic field B_0 on the Zeeman energy-level spacing, we note that in both the $6^2S_{1/2}(F_g=1)$ state and the $6^2P_{3/2}(F_e=2)$ state of our fictitious isotope the Zeeman splitting is 1.4 MHz/G. We model our optical field as a singlemode diode laser (i.e., a phase-diffusion field with small relative intensity noise), and for the work reported here we always set $\beta=10^3\gamma_L$. Unless otherwise noted, the parameters of Table I are employed in all of the numerical experiments.

We write the density matrix evolution as

$$\dot{\sigma}=-\frac{i}{\hbar}[(H_0+V),\sigma]+\Gamma(\sigma), \tag{18}$$

TABLE I. Parameters used in the numerical computations of an alkalilike (i.e., cesiumlike) beam interacting with a nonstationary stochastic field

Parameter	Value
Einstein-A coefficient A_{eg}	5.16 MHz
Initial population in $F_g=1$ ground state σ_0	0.75
Saturation intensity I_s	13.1 mW/cm^2
Ground- and excited-state Zeeman splitting	1.4 MHz/G
Oven temperature	100 °C
Most probable atomic speed v_{mp}	2.2×10^4 cm/sec
Field-atom interaction length L	0.4 cm
Static magnetic field B_0	500 mG
Laser intensity I	25 mW/cm^2
Laser frequency's modulation amplitude $m\omega_m/2\pi$	2 MHz
Laser linewidth γ_L	1 MHz
Laser line shape wing parameter β	$10^3\gamma_L$
Laser $\delta I_{\rm rms}/\langle I\rangle$	10^{-6}

where the perturbation V on the right-hand-side of Eq. (18) corresponds to laser excitation with

$$V(t)=-\vec{\mu}\cdot\vec{E}(t)=-\frac{1}{2}(\vec{\mu}\cdot\hat{x})E_0(e^{i\omega t}+e^{-i\omega t}), \tag{19}$$

and the last term on the right-hand side of Eq. (18) corresponds to spontaneous emission. (As usual, we make the rotating-wave approximation in solving these equations.) Here, H_0 is the atomic Hamiltonian in the absence of the optical field, which includes the atom's static magnetic-field interaction; E_0 and ω are the laser electric-field strength and frequency, respectively, such that $E_0=\langle E_0\rangle[1+\zeta(t)]$ and $\omega=\langle\omega\rangle+\delta(t)$. For these random processes, the $\delta(t)$ correlation function is given by Eq. (4), and for $\zeta(t)$ [with $\langle\zeta(t)\rangle=0$] we have

$$\langle\zeta(t)\zeta(t+\tau)\rangle=\gamma_L\tau_\zeta\exp\left(-\frac{|\tau|}{\tau_\zeta}\right). \tag{20}$$

In Eq. (20), τ_ζ is related to the relative intensity noise (RIN) of the laser in a 1-Hz bandwidth (i.e., we define RIN as $\delta I_{\rm rms.}/\langle I\rangle$) such that $\delta I_{\rm rms}/\langle I\rangle=4\tau_\zeta\sqrt{\gamma_L}$.

Following Cohen-Tannoudji [25], the matrix elements of the spontaneous emission term are given by

$$\langle F_e m_e|\Gamma|F_e m_e'\rangle=-A_{eg}\langle F_e m_e|\sigma|F_e m_e'\rangle, \tag{21a}$$

$$\langle F_e m_e|\Gamma|F_g m_g\rangle=-\frac{A_{eg}}{2}\langle F_e m_e|\sigma|F_g m_g\rangle, \tag{21b}$$

and

$$\langle F_g m_g|\Gamma|F_g m_g'\rangle = A_{eg}[J_e][F_g][F_e]\begin{Bmatrix} J_e & F_e & I \\ F_g & J_g & 1 \end{Bmatrix}^2 \times\left[\sum_{q,m_e,m_e'}(-)^{2F_g+q-m_g-m_e'}\begin{pmatrix} F_g & 1 & F_e \\ -m_g & q & m_e \end{pmatrix}\times\begin{pmatrix} F_g & 1 & F_e \\ -m_g' & q & m_e' \end{pmatrix}\langle F_e m_e|\sigma|F_e m_e'\rangle\right], \quad (21c)$$

where $[K]\equiv(2K+1)$. Since, in general, atomic coherences play an important role in the laser-induced generation of LIF noise (e.g., the atomic absorption cross section is defined by the imaginary part of certain off-diagonal density matrix elements), it is worth stating explicitly that according to Eq. (21c), atomic coherences among the excited state Zeeman sublevels do not simply disappear as a result of spontaneous decay; they are to some extent transferred to the ground state [26].

Solving the density matrix equations numerically, we compute the temporal evolution of three physical quantities: two moments of the ground-state population distribution [27] (i.e., the dipole moment corresponding to ground state orientation, $\langle F_{g,z}\rangle$ and the quadrupole moment corresponding to ground-state alignment $\langle 3F_{g,z}^2-F_g^2\rangle$) and the total-excited state population ρ_e. Since the fluorescence signal is proportional to ρ_e, the fluctuations in ρ_e relative to its average value constitute our measure of the LIF signal-to-noise ratio. We determine the noise at an averaging time of one second using the Allan variance [17], so that our signal-to-noise ratios correspond to values in a one-hertz bandwidth. Further details of the numerical computations may be found in the appendix.

Figure 3 shows the average values of orientation, alignment and fluorescence, along with the standard errors of a one-second average, as a function of laser detuning; the nominal conditions of Table I apply except for $I=120\ \mu\mathrm{W/cm}^2$, $\omega_m=0$ and $B_0=0$. Figure 4 shows the same quantities and nominal Table I conditions except for $I=100\ \mu\mathrm{W/cm}^2$ (i.e., $\omega_m\neq 0$ and $B_0\neq 0$). In the case of Fig. 3, where we have a weak optical field, no modulation and no Zeeman splitting, there is a complete absence of polarization in the ground state, though an alignment does develop due to our excitation with $\pm\sigma$ polarized light. Further, the full width at half maximum (FWHM) of the fluorescence is 5.95 MHz, which is within 4% of the expected result for a two-level atom (i.e., $A_{eg}+\gamma_L$ [28]). Note that the standard error in the alignment and fluorescence has a minimum on resonance as one might expect from the adiabatic approximation.

Examining Fig. 4, we see that as a consequence of the nonzero magnetic field, the ground state develops a polarization when the laser is off resonance. Moreover, in combination with the nonzero laser modulation the alignment and fluorescence signals broaden (i.e., the fluorescence FWHM is now 8.04 MHz). Note that the standard error of the fluorescence no longer has a minimum on resonance, but has a much more complicated appearance. Notwithstanding these

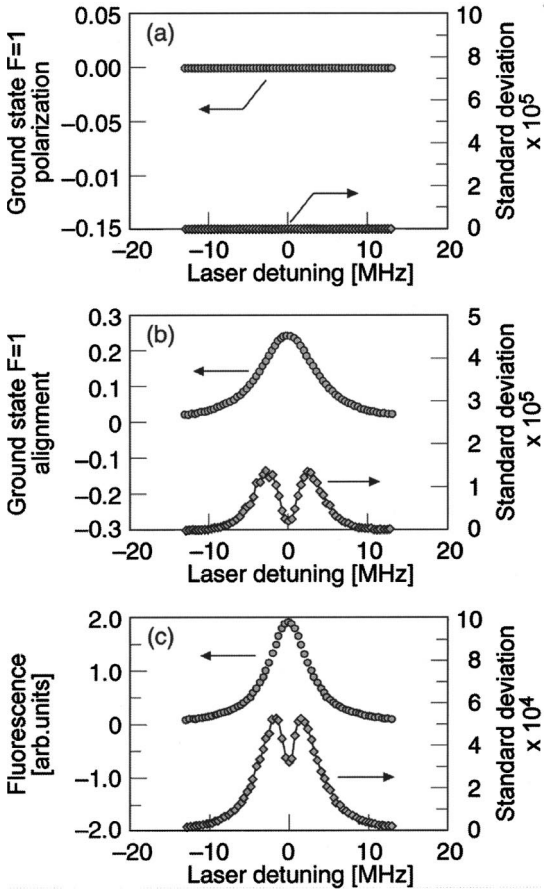

FIG. 3. (a) Ground-state ($F=1$) polarization, (b) ground-state ($F=1$) alignment, and (c) fluorescence (arbitrary units) for a numerical experiment with the nominal conditions of Table I except for $I=120\ \mu\mathrm{W/cm}^2$, $\omega_m=0$, $m=0$, and $B_0=0$.

observations, the important point to notice from Figs. 3 and 4 is that the nonzero polarization and nonzero alignment imply that optical pumping occurs in this system, even though we are dealing with a cycling transition. Consequently, as the laser frequency randomly deviates from its average value, LIF fluctuations will arise from stochastic variations in the excitation efficiency *and* stochastic variations in the moments of the ground state's population distribution. This coupling of excitation efficiency and optical pumping is not captured in analyses that are limited to two-level atoms, though it is a complication that arises in real multilevel atoms.

IV. RESULTS OF THE NUMERICAL EXPERIMENTS

Influence of field nonstationarity on long-term LIF noise. Figure 5 shows the Allan deviation of the fractional fluorescence fluctuations $\sigma_{\Delta F/F}(\tau)$, as a function of averaging time τ. In Fig. 5(a) we consider weak-field conditions (i.e., $I/I_s\sim 0.01$), while in Fig. 5(b) we consider strong-field conditions (i.e., $I/I_s\sim 2$); all other parameters are as listed in Table I. In each figure, the solid line corresponds to the case of no laser-frequency modulation, while the data points and dashed line correspond to LIF noise in the presence of the nonstationary field. There are two points to note with regard to Fig.

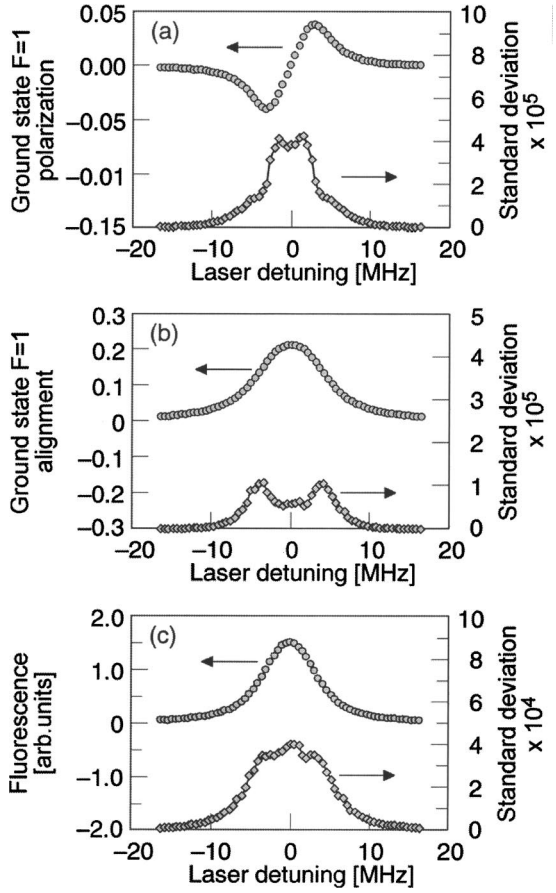

FIG. 4. (a) Ground-state ($F=1$) polarization, (b) ground-state ($F=1$) alignment, and (c) fluorescence (arbitrary units) for a computer experiment with the nominal conditions of Table I except for $I=100\ \mu\mathrm{W/cm^2}$.

5. First, independent of laser intensity, the nonstationary character of the field has a dramatic effect on the Allan deviation, increasing the LIF noise by about 200% for the figures' specific conditions. Additionally, even though the field is nonstationary, the LIF noise is white (i.e., the Allan deviation decreases with averaging time as $\sqrt{\tau}$) as predicted by the adiabatic approximation. As previously noted within the adiabatic approximation, $\sigma^2_{\Delta F/F}(\tau)$ corresponds to a mean square of the fluorescence fluctuations averaged over a modulation period. Since the field is periodically stationary, the averaging gives the LIF fluctuations stationary character, and for averaging times much greater than the modulation period the nonstationary character of the field simply amplifies the white-noise level of the LIF.

Signal-to-noise ratio and laser-frequency modulation amplitude. Figure 6 shows the signal-to-noise ratio of the LIF ($\Delta_0=0$) as a function of laser-frequency modulation amplitude $m\omega_m$, where the ''signal'' corresponds to the dc level of fluorescence [29]. Diamonds correspond to $\omega_m/2\pi=100$ kHz; circles correspond to $\omega_m/2\pi=1$ MHz, and triangles correspond to $\omega_m/2\pi=10$ MHz. As predicted by the adiabatic approximation, for $\omega_m<A_{eg}$, the S/N ratio does not depend so much on the value of the modulation frequency, but on the amplitude of the laser-frequency modulation $m\omega_m$.

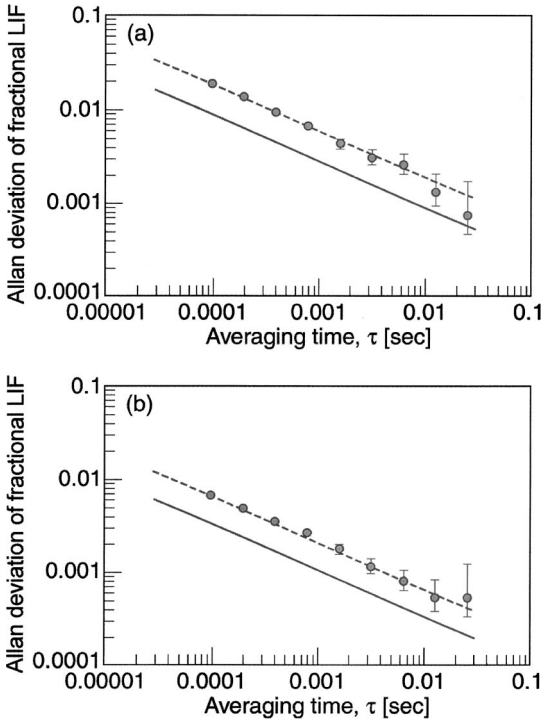

FIG. 5. Allan deviation of the fractional fluorescence fluctuations $\sigma_{\Delta F/F}(\tau)$ for the laser tuned on resonance (i.e., $\Delta_0=0$): (a) $I=100\ \mu\mathrm{W/cm^2}$, (b) $I=25\ \mathrm{mW/cm^2}$; all other parameters as in Table I. In each graph the solid line corresponds to LIF without laser-frequency modulation while the data points correspond to LIF with laser-frequency modulation.

Though the S/N ratio for $\omega_m/2\pi=10$ MHz remains relatively high for a range of modulation amplitudes (i.e., $m\omega_m/2\pi\leqslant 5$ MHz), one should interpret this result cautiously. Basically, at this very high modulation frequency the atoms' response is nonadiabatic, implying that the atoms do not easily follow the laser's deterministic frequency varia-

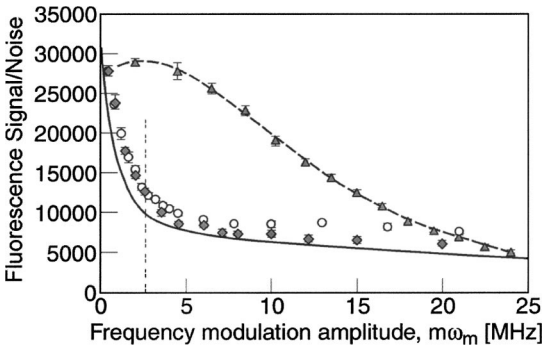

FIG. 6. LIF signal-to-noise ratio for the laser tuned to resonance as a function of the laser-frequency modulation amplitude; parameters are given in Table I except as noted: diamonds correspond to $\omega_m/2\pi=100$ kHz, circles correspond to $\omega_m/2\pi=1$ MHz, and triangles correspond to $\omega_m/2\pi=10$ MHz. The long dashed line running through the triangles is simply an aid to guide the eye, while the vertical double-dashed line indicates $m\omega_m=A_{eg}$. The solid line represents the signal-to-noise ratio predicted by the adiabatic approximation.

tions. Hence, it is not surprising that the noise is relatively low. Nevertheless, the laser's frequency is modulated with intent, presumably to generate an ac signal that can be used to stabilize the laser wavelength. If the modulated signal is derived from the atomic beam's LIF, then nonadiabaticity implies that the ac signal will be small, possibly negating any positive influence of the fast frequency modulation on the (dc) signal-to-noise ratio. However, if the correction signal for laser stabilization were derived from a separate atomic system with a broader atomic bandwidth (e.g., LIF from an atomic vapor), then it might be possible to take advantage of nonadiabaticity to improve the S/N of the atomic beam's LIF while maintaining a large ac signal for laser stabilization purposes.

In order to proceed further with the interpretation of the numerical results, we define the adiabatic fluorescence signal F_a as $A_{eg}\overline{T}_{\rm fl}[\overline{\sigma_{22}^{(0)}}]_T$, where $\overline{T}_{\rm fl}$ is the most-probable flight time of the atoms through the laser-atom interaction region. Then, solving Eqs. (10) for $[\overline{\sigma_{22}^{(0)}}]_T$ we obtain

$$F_a=\frac{\frac{1}{2}A_{eg}\overline{T}_{\rm fl}\sigma_0\left(\frac{\gamma_2}{\gamma_1}\right)\left(\frac{I}{2I_s}\right)A_{eg}^2}{\sqrt{\left[\gamma_2^2+\Delta_0^2+\left(\frac{\gamma_2}{\gamma_1}\right)\left(\frac{I}{2I_s}\right)A_{eg}^2\right]\left[\gamma_2^2+\Delta_0^2+m^2\omega_m^2+\left(\frac{\gamma_2}{\gamma_1}\right)\left(\frac{I}{2I_s}\right)A_{eg}^2\right]}}. \tag{22}$$

From the parameters of Table I, and with $\gamma_2=1/2(A_{eg}+\gamma_L)$, we find that $F_a=135$, which is within about 5% of the numerical adiabatic result of $F_a=129$. (For the nominal 500 mG field, the several ground-to-excited state transitions are shifted by ± 0.7 MHz.) In order to compute the signal-to-noise ratio, we now recognize that Zeeman shifts of the resonant transitions will cause the noise to be dominated by N_Δ at small values of $m\omega_m$. For conceptual purposes, we therefore write the S/N ratio as

$$(S/N)\cong\frac{F_a}{A_{eg}\overline{T}_{\rm fl}(N_0+N_\Delta)}. \tag{23}$$

Substituting from Eqs. (17a), (17b), and (22), and using the parameters of Table I [30], we get the solid curve of Fig. 6 for the noise in a one hertz bandwidth. As expected, at low modulation amplitudes the agreement between the numerical results and the adiabatic approximation is quite good, showing in both cases a rapid fall off in S/N up to approximately $m\omega_m/2\pi\sim 5$ MHz. Even the leveling-off of the S/N ratio for $m\omega_m/2\pi\geqslant 5$ MHz is captured by the adiabatic approximation, though its validity conditions are clearly violated. Note that if we had not included the N_Δ term in Eq. (23), ignoring for the sake of argument effects of shot noise, the signal-to-noise ratio would have diverged at low modulation amplitudes, which suggests that the Zeeman splitting of a multilevel atom can play an important role in determining LIF noise.

Signal-to-noise ratio and Zeeman splitting. As suggested by the results shown in Fig. 6 at low modulation amplitudes, the multilevel nature of the stochastic-field–atom interaction problem can have a significant influence on the S/N ratio. To explore this issue further, we examined the S/N ratio as a function of Zeeman splitting $\Delta_{\rm Zeeman}$. The results are shown in Fig. 7(a), where diamonds correspond to $m\omega_m/2\pi=2$ MHz and circles correspond to $m\omega_m/2\pi=0$; all other parameters except for magnetic-field strength correspond to Table I values. What is striking about the results is that for a limited range of magnetic-field strengths the S/N ratio increases dramatically (i.e., between 300 and 400%); and as shown in Fig. 7(b), where we plot the signal and noise separately, the effect appears to be due to a strong reduction in LIF noise over this particular range of $\Delta_{\rm Zeeman}$.

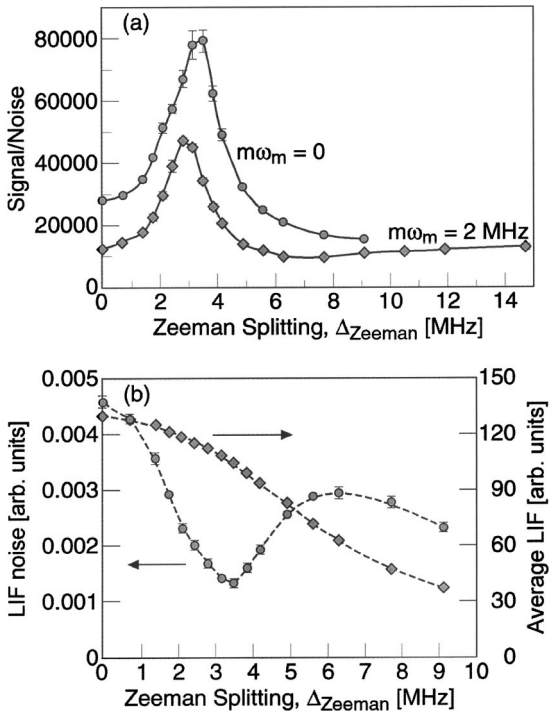

FIG. 7. (a) Signal-to-noise ratio as a function of Zeeman splitting as determined in the computations by the magnetic field strength ($\Delta_0=0$); parameters for the calculation are as indicated in Table I except for the modulation amplitude. (b) LIF signal and noise plotted separately for $m\omega_m=0$, showing that the enhancement in the S/N ratio is driven by a decrease in LIF noise.

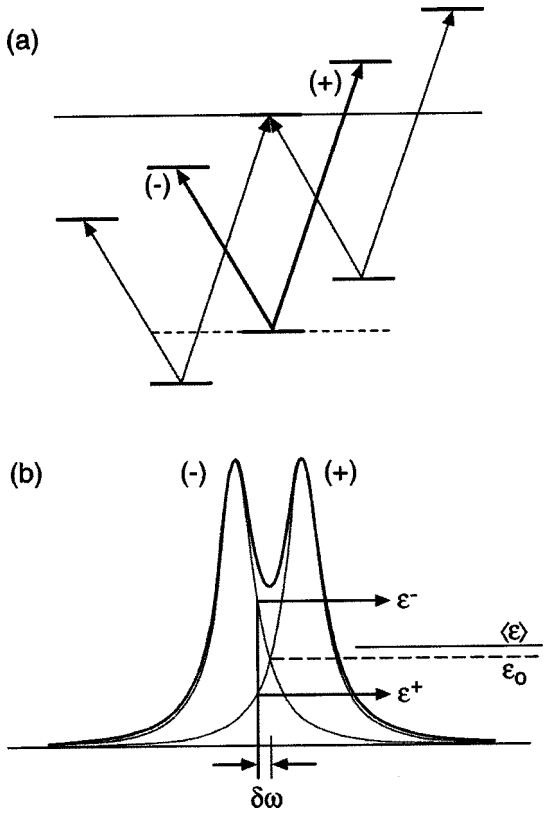

FIG. 8. (a) Illustration of the multiple V systems in the present problem. (b) Illustration of the manner in which LIF noise might be suppressed in a V system as discussed in the text.

As a working hypothesis to explain the increase in the S/N ratio, we first recognize that because of the multilevel nature of the problem and the laser's polarization, we are dealing with multiple situations of V-system excitation as drawn in Fig. 8(a). Consequently, as illustrated in Fig. 8(b), when the Zeeman splitting is not too large the (nominally on-resonance) laser excites two coherently coupled transitions; these are offset from the laser frequency by $+|\Delta_{\mathrm{Zeeman}}|$ and $-|\Delta_{\mathrm{Zeeman}}|$, with the average excitation efficiency for the two branches of the V system given by ε_0. If the laser frequency randomly decreases by $\delta\omega$, the excitation efficiency for the $(-)$ branch of the V system increases to ε^-, while the excitation efficiency for the $(+)$ branch decreases to ε^+. Though individually the excitation efficiencies for the $(-)$ and $(+)$ branches may change dramatically, the overall excitation efficiency (giving rise to the LIF signal) might only change slightly from ε_0 to $\langle\varepsilon\rangle$. Consequently, we argue that the V system has built into it an intrinsic ability to mitigate PM-to-AM conversion noise in the LIF signal. This is consistent with Eq. (17b), where N_Δ for a two-level system depends on the sign of Δ. In order to explain the appearance of Fig. 7(a), we note that at small Zeeman splittings the multiple V systems are degenerate; thus the noise cancellation property of the V system is attenuated and the atom produces LIF noise in the manner of a two-level atom. At somewhat stronger magnetic-field strengths, with the Zeeman degeneracy lifted, the V system's intrinsic noise mitigation process becomes effective, giving rise to an enhanced S/N ratio. At relatively high values of the magnetic-field strength, where the computations of Fig. 7(b) indicate an increase in LIF noise, the situation is less clear. Qualitatively, it seems reasonable to presume that an inherent noise-mitigation property of the V system becomes less effective as the $(-)$ and $(+)$ branches take on independent-transition character, as would occur at very large values of the Zeeman splitting.

V. SUMMARY

In this work we have investigated the interaction of a nonstationary field with a multilevel atom. In particular, we examined the fluctuations in laser-induced fluorescence from an alkali-metal-like atom when it interacts with a singlemode field undergoing deterministic frequency modulation (i.e., a periodically stationary field). Two of our key findings are that (1) though at low Fourier frequencies the nonstationary (i.e., modulated) character does not appear explicitly in the LIF fluctuations, it does amplify their (white-noise) magnitude and (2) in the adiabatic regime of the stochastic-field–atom interaction the important modulation parameter is the amplitude of the deterministic frequency excursions (i.e., $m\omega_m$). Additionally, for the multilevel atom we found that the LIF noise is significantly reduced at a critical value of the Zeeman splitting. Though we developed a heuristic explanation for the phenomenon, an accurate understanding of its origin will require a more careful analytical examination of LIF noise in a V system. As is well known, V systems and Λ systems are subtle, leading to effects such as coherent-population trapping and electromagnetically induced transparency [31]. Notwithstanding the physical origin of the critical decrease in LIF noise, its observation may have important implications for precision spectroscopy. Specifically, in the area of atomic clocks, where short-term frequency stability is typically determined by the S/N ratio, the present results suggest that operation of a beam clock at an appropriate magnetic-field strength could lead to factors of 3 to 5 improvement in frequency stability. It will be interesting to see if this prediction holds true for the next generation of compact cesium beam clocks employing diode lasers for optical pumping and LIF detection [32].

ACKNOWLEDGMENTS

The author would like to thank R. Lutwak for several stimulating discussions regarding various aspects of the nonstationary, stochastic-field–atom interaction problem. This work was supported by U. S. Air Force Space and Missile Systems Center under Contract No. F040701-00-C-0009.

APPENDIX

In our numerical algorithm, we run a ''fast'' time scale and a ''slow'' time scale. Basically, the fast time scale corresponds to a specific ensemble of atoms' temporal evolution as it crosses the field-atom interaction region, while the slow time scale corresponds to the bandwidth of the measurement system. For some particular moment of the slow time scale t_s we consider the propagation of an ensemble of atoms

through the field-atom interaction region, with the ensemble composed of a number of different velocity groups [i.e., we consider our ensemble as the set $\{\sigma(v)\}$]. Each member of the set corresponds to a subensemble of atoms in one of ten different velocity groups. We begin by generating a realization of our random field [33], and for each velocity group we solve the density matrix equations over the group's laser-atom interaction time L/v; here, L is the length of the interaction region and v is the atomic speed for the particular velocity group. (Our minimum atomic velocity $v_{\min}$ equals 4×10^3 cm/sec and our maximum equals $2.7v_{mp}$, where v_{mp} is the most probable velocity for a given alkali-oven temperature.) The density matrix equations are solved using a variable step-size fourth-order Runge-Kutta-Fehlberg routine [34], and each atomic velocity group in the set sees the same realization of the field. For each velocity group we integrate the fluorescence signal $F(t_s,v,t_f) = A_{eg}\rho_e(t_s,v,t_f)$, over the interaction time t_{int} and also record the values of ground state dipole and quadrupole population distributions $\rho_d(t_{\text{int}},v)$ and $\rho_q(t_{\text{int}},v)$ respectively, as the atomic velocity groups exit the field-atom interaction region. Using Gaussian quadrature [35] to numerically integrate over the velocity distribution for the thermal beam [36], we obtain $\rho_d(t_s)$, $\rho_q(t_s)$, and $F(t_s)$.

At each value of the slow time we generate a new realization. Since these realizations are uncorrelated, we are essentially assuming that the bandwidth of the measurement system corresponds to a timescale that is long compared to the field's correlation time. We basically consider our determinations of $\rho_d(t_s)$ and $\rho_q(t_s)$ as the outputs of a zero-order sample-and-hold [37] of duration T_{fl}, sampling at the rate $0.1/T_{\text{fl}}$, where T_{fl} is the maximum flight time through the interaction region (i.e., $L/v_{\min}$). We analyze the time series of these sample-and-hold outputs, or the fluorescence $F(t_s)$, which is an average over T_{fl}, using the Allan variance. [Note that our instantaneous values of $\rho_d(t_s)$ and $\rho_q(t_s)$ are unbiased estimates of the average values of these quantities over the duration T_{fl}.] Though our simulation corresponds to measurements with ''dead time,'' since the sampling time is ten times longer than the averaging time T_{fl}, the dead-time bias function is unity because the LIF stochastic process corresponds to white noise [38].

[1] P. Lambropoulos, C. Kikuchi, and R. K. Osborn, Phys. Rev. **144**, 1081 (1966); C. Lecompte, G. Mainfray, C. Manus, and F. Sanchez, Phys. Rev. A **11**, 1009 (1975); J. H. Eberly, Phys. Rev. Lett. **37**, 1387 (1976).

[2] P. Avan and C. Cohen-Tannoudji, J. Phys. B **10**, 155 (1977).

[3] See, for example, H. Kimble and L. Mandel, Phys. Rev. A **15**, 689 (1977); P. L. Knight, W. A. Molander, and C. R. Stroud, Jr., *ibid.* **17**, 1547 (1978); A. T. Georges and S. N. Dixit, *ibid.* **23**, 2580 (1981), and references therein.

[4] M. H. Anderson, R. D. Jones, J. Cooper, S. J. Smith, D. S. Elliott, H. Ritsch, and P. Zoller, Phys. Rev. Lett. **64**, 1346 (1990); M. H. Anderson, R. D. Jones, J. Cooper, S. J. Smith, D. S. Elliott, H. Ritsch, and P. Zoller, Phys. Rev. A **42**, 6690 (1990).

[5] J. C. Camparo and P. Lambropoulos, Opt. Commun. **85**, 213 (1991); M. P. van Exter, D. M. Boersma, A. K. Jansen van Doorn, and J. P. Woerdman, Phys. Rev. A **49**, 2861 (1994); J. C. Camparo, *ibid.* **54**, 410 (1996).

[6] T. Yabuzaki, T. Mitsui, and U. Tanaka, Phys. Rev. Lett. **67**, 2453 (1991).

[7] R. J. McLean, P. Hannaford, C. E. Fairchild, and P. L. Dyson, Opt. Lett. **18**, 1675 (1993); D. H. McIntyre, C. E. Fairchild, J. Cooper, and R. Walser, *ibid.* **18**, 1816 (1993).

[8] J. C. Camparo, J. Opt. Soc. Am. B **15**, 1177 (1998); J. C. Camparo and J. G. Coffer, Phys. Rev. A **59**, 728 (1999).

[9] J. G. Coffer, M. Anderson, and J. C. Camparo, Phys. Rev. A **65**, 033807 (2002).

[10] J. C. Camparo and W. F. Buell, in *Proceedings of the 1997 IEEE Frequency Control Symposium* (IEEE Press, Piscataway, NJ, 1997), pp. 253–258; G. Mileti, J. Deng, F. L. Walls, D. A. Jennings, and R. E. Drullinger, IEEE J. Quantum Electron. **34**, 233 (1998).

[11] Investigations of multiphoton processes in pulsed fields is an obvious exception. See, for example, V. N. Bagratashvili, S. I. Ionov, G. V. Mishakov, V. A. Semchishen, and A. V. Masalov, J. Opt. Soc. Am. B **4**, 129 (1987); J. C. Camparo and P. Lambropoulos, Opt. Lett. **19**, 1562 (1994); J. C. Camparo and P. Lambropoulos, Opt. Commun. **137**, 413 (1997).

[12] Though such a field falls within the broad classification of a nonstationary stochastic process, it may be worth noting that this particular field has the special characteristic of being periodically stationary in the wide sense. See A. Papoulis, *Probability, Random Variables and Stochastic Processes* (McGraw-Hill, New York, 1965), Chap. 9.

[13] R. S. Eng, J. F. Butler, K. J. Linden, Opt. Eng. **19**, 945 (1980); H. Groll, Ch. Schnürer-Patschan, Yu. Kuritsyn, and K. Niemax, Spectrochim. Acta, Part B **49**, 1463 (1994).

[14] W. Lenth, Opt. Lett. **8**, 575 (1983); F. S. Pavone and M. Inguscio, Appl. Phys. B: Photophys. Laser Chem. **56**, 118 (1993).

[15] See, for example, D. Wang, L. Xie, and Y. Wang, Opt. Lett. **13**, 820 (1988); T. Ikegami, S-I. Ohshima, Y. Nakadan, and Y. Koga, Rev. Sci. Instrum. **61**, 3719 (1990).

[16] R. Lutwak (private communication); R. Lutwak, D. Emmons, R. M. Garvey, and P. Vlitas, in *Proceedings of the 33rd Annual Precise Time and Time Interval (PTTI) Systems and Applications Meeting* (U.S. Naval Observatory, Washington DC, 2001), pp. 19–32.

[17] Basically, the Allan deviation corresponds to the standard error of the LIF signal for some averaging time, and is similar to the Kolmogorov structure function. The advantage of the Allan deviation for the analysis of time-series is that it converges for some important colored noise processes. For further discussion, see J. Rutman, Proc. IEEE **66**, 1048 (1978), and D. W. Allan, IEEE Trans. Instrum. Meas. **IM-36**, 646 (1987).

[18] For a pure phase-diffusion field, the frequency fluctuations have a white spectral density $S_\delta(f)$ which implies that their variance σ_δ^2 is infinite: $\sigma_\delta^2 = \int_{-\infty}^{\infty} S_\delta(f)\,df$. However, since the

time scale of the field-atom coupling is on the order of Ω^{-1}, the atom essentially responds to an average frequency fluctuation over this time interval, which places what amounts to a high frequency cutoff on the spectral density. Thus, with regard to the field atom interaction we expect $\sigma_\delta^2 \approx 2\int_0^{\Omega/2\pi} S_\delta(f)\,df$, which has a finite and possibly small value.

[19] P. Zoller and P. Lambropoulos, J. Phys. B **12**, L547 (1979).

[20] The β parameter basically causes the wings of the laser line shape to fall off faster than a Lorentzian.

[21] J. C. Camparo, Contemp. Phys. **26**, 443 (1985).

[22] A. S. Pazgalev and N. N. Yakobson, Opt. Spectrosc. **77**, 622 (1994); R. P. Frueholz and J. C. Camparo, Phys. Rev. A **54**, 3499 (1996).

[23] J. Kitching, S. Knappe, N. Vukicević, L. Hollberg, R. Wynands, and W. Weidmann, IEEE Trans. Instrum. Meas. **49**, 1313 (2000).

[24] Though Cs^{125}, Cs^{127}, and Cs^{129} all have nuclear spin $\frac{1}{2}$, their lifetimes are 45 min, 6.2 h, and 32 h, respectively. For completeness we note that these isotopes' nuclear magnetic moments are $+1.41$, $+1.46$, and $+1.48$ nuclear magnetons, respectively, while that of Cs^{133} is $+2.58$ nuclear magnetons.

[25] C. Cohen-Tannoudji, in *Les Houches Session XXVII, 1975, Vol. 1 of Frontiers in Laser Spectroscopy Volume 1* (North-Holland, Amsterdam, 1977), pp. 3–104.

[26] This is especially noteworthy in the case of our fictitious isotope, where the excited and ground-state Zeeman coherences evolve at the same rate, since the Zeeman splittings of the ground and excited states are equal. However, in the real Cs^{133}, atom where the excited and ground state Zeeman splittings are 560 KHz/G and 350 KHz/G, respectively, one would expect the importance of this term to be diminished when atomic evolution is examined on a time scale that is long compared to the beat frequency between the two sets of coherences. In future work it will be interesting to more carefully examine the importance of this term in the PM-to-AM conversion process.

[27] K. Blum, *Density Matrix Theory and Applications* (Plenum, New York, 1981), Chap. 4; W. E. Baylis, in *Progress in Atomic Spectroscopy: Part B* (Plenum, New York, 1979) Ch. 28.

[28] A. T. Georges and P. Lambropoulos, Phys. Rev. A **18**, 587 (1978).

[29] In order to simplify the interpretation of our results, the present work restricts attention to dc signals, as would be of interest in double-resonance experiments where the laser is modulated in order to stabilize its wavelength and the signal of interest corresponds to a change in LIF as some other field is varied. In future work, we plan to consider the case of S/N ratios for the ac signal at $f=\omega_m$.

[30] In order to evaluate Eqs. (17a) and (17b), we need to evaluate $\sqrt{\langle \overline{\delta_\tau^2} \rangle}$. For a phase-diffusion field, we have from Eq. (5) in a bandwidth B (as opposed to the bandwidth Ω set by the atom), $\langle \overline{\delta_B^2} \rangle = (2/\pi)\gamma_L \beta \tan^{-1}(B/2\beta)$. Thus, for noise in a one hertz bandwidth (i.e., $\tau^{-1}=B=2\pi$ and $\beta \gg B$) $\langle \overline{\delta_\tau^2} \rangle = 2\gamma_L$ (rad/sec).

[31] M. O. Scully and M. S. Zubairy, *Quantum Optics* (Cambridge University Press, Cambridge, 1997).

[32] See, for example, P. Gill, *Proceedings of the 6th Symposium on Frequency Standards and Metrology* (World Scientific, New Jersey, 2002).

[33] J. C. Camparo and P. Lambropoulos, Phys. Rev. A **47**, 480 (1993); J. C. Camparo and P. Lambropoulos, J. Opt. Soc. Am. B **9**, 2163 (1992).

[34] W. H. Press and S. A. Teukolsky, Comput. Phys. **6**, 188 (1992); W. Cheney and D. Kincaid, *Numerical Mathematics and Computing* (Brooks/Cole, Monterey, CA, 1985), Chap. 8.

[35] P. J. Davis and I. Polonsky, in *Handbook of Mathematical Functions*, edited by M. Abramowitz and I. A. Stegun *National Bureau of Standards Applied Mathematics Series 55* (National Bureau of Standards, Washington, DC, 1964).

[36] N. F. Ramsey, *Molecular Beams* (Oxford University Press, Oxford, 1956), Chap. 2.

[37] J. R. Ragazzini and G. F. Franklin, *Sampled-Data Control Systems* (McGraw-Hill, New York, 1958), Chap. 3.

[38] D. W. Allan, J. H. Shoaf, and D. Halford, in *Time and Frequency: Theory and Fundamentals*, edited by B. E. Blair, *National Bureau of Standards Monograph 140* (National Bureau of Standards, Washington, DC, 1974).